

## Wetting transitions of classical liquid films: A nearly universal trend

E. Cheng

*Department of Physics, Pennsylvania State University, University Park, Pennsylvania 16802  
and Division de Physique Théorique, Institut de Physique Nucléaire, 91406 Orsay Cedex, France*

M. W. Cole

*Department of Physics, Pennsylvania State University, University Park, Pennsylvania 16802*

W. F. Saam

*Department of Physics, The Ohio State University, Columbus, Ohio 43210*

J. Treiner

*Division de Physique Théorique, Institut de Physique Nucléaire, 91406 Orsay Cedex, France  
and Laboratoire d'Acoustique et Optique de la Matière Condensée, Tour 13, Boîte 86, 4 place Jussieu,  
75252 Paris Cedex 05, France*

(Received 15 July 1993)

We calculate wetting behavior for the adsorption of Ne, Ar, Kr, and Xe for temperatures above their triple point. Experimental observations of wetting transitions of these simple liquids are predicted. We also report a nearly universal trend in the physical interaction parameters for Ar, Kr, and Xe on various substrates. With a simple model, we show that the classical "law of corresponding states" can be extended to predict approximately universal behavior in the wetting transitions of these films. We then demonstrate, by comparison with Ne, H<sub>2</sub>, and He films, that quantum effects enhance wetting in that there is a larger range of adsorption parameters leading to wetting when zero-point motion is included.

### I. INTRODUCTION

The recent prediction and subsequent experimental observation of wetting transitions, along with associated prewetting transitions, of <sup>4</sup>He and H<sub>2</sub> on Cs and Rb surfaces<sup>1-5</sup> have refocused much attention on the problem of wetting transitions.<sup>6</sup> Indeed, the study of wetting transition phenomena, proposed some fifteen years ago,<sup>7</sup> has reached a period of exciting development with the introduction of quantum films and weak-binding substrates.<sup>1,5</sup>

In this paper, we extend our theoretical study of quantum films<sup>1,5</sup> to classical ones and show that similar wetting behavior and transitions of simple gases on weak-binding surfaces such as alkali metals should also be observable here. Furthermore, after observing a nearly universal trend in the physical interactions involving classical inert gases and various surfaces, we suggest an approximate universality in the wetting transitions of physically adsorbed classical films. This universality is similar to, and in fact partly based on, the classical "law of corresponding states" (LCS) in the bulk fluid.<sup>8</sup> If confirmed by experiments, our result can be viewed as an extension of the LCS to the field of wetting transitions.

### II. MODEL CALCULATIONS

It is well understood that the competition between the adsorbate-substrate and the adsorbate-adsorbate in-

teractions plays a crucial role in determining wetting properties.<sup>6</sup> A very simple and approximate model based on the energy balance of these interactions has been proposed and used to study the wetting properties of <sup>4</sup>He films. It was found to be surprisingly accurate, based on a comparison with a more sophisticated density functional calculation.<sup>1</sup> According to this model, wetting occurs when the surface free energy cost is sufficiently offset by the potential energy gain from the substrate's attraction:<sup>9</sup>

$$\hat{\sigma}_{sl} + \sigma_{lv} + n \int_{z_m}^{\infty} dz V(z) \leq 0. \quad (1)$$

Here  $\sigma_{lv}$  and  $n$  are the bulk liquid-vapor surface tension and liquid number density of the film,  $\hat{\sigma}_{sl}$  is the free energy cost internal to the liquid of creating the substrate-liquid interface, and  $z_m$  is the minimum of the substrate potential well  $V(z)$ . We will henceforth approximate  $\hat{\sigma}_{sl}$  by  $\sigma_{lv}$ . This may slightly underestimate  $\hat{\sigma}_{sl}$  since the substrate-film interface is expected to be stiffer, and hence less prone to thermal excitation, than the liquid-vapor interface.<sup>10</sup>

The substrate potential  $V(z)$  is here characterized by two parameters, the well depth  $D$  and the coefficient of long range van der Waals attraction  $C_3$ . We adopt the simple Lennard-Jones model potential form<sup>11</sup>

$$V(z) = \frac{4C_3^3}{27D^2z^9} - \frac{C_3}{z^3}. \quad (2)$$

The wetting condition (1) then becomes

$$(C_3 D^2)^{1/3} \geq 3.33 \sigma_{lv}(T)/n(T). \quad (3)$$

This relation becomes an equality when the temperature  $T$  is equal to the wetting transition temperature  $T_w$ . This simple model has been applied to liquid  $^4\text{He}$  (Ref. 1) and  $\text{H}_2$  (Ref. 5) films to predict  $T_w$  on those alkali metal surfaces which are not wetted by  $^4\text{He}$  and  $\text{H}_2$  at  $T = 0$  and the bulk triple temperature  $T_t$ , respectively. The semi-quantitative success in these previous cases<sup>1,5</sup> leads us to believe that it should also be applicable here. We observe that the left side of Eq. (3) contains information characterizing the adsorbate-substrate interaction while its right side involves implicitly the adsorbate-adsorbate interaction. The competition between the two interactions determines the wetting transition.

Much effort has been expended in the study of these two kinds of interactions, both theoretically and experimentally.<sup>12,13</sup> This has resulted in a set of reasonably accurate potentials, although the adsorption data base is generally less complete and accurate than that of the interatomic forces. We present some of the available data for the parameters  $C_3$  and  $D$  of inert gases of Ne, Ar, Kr, and Xe on various surfaces in Tables I and II. With the information concerning  $\sigma_{lv}(T)$  and  $n(T)$  in Ref. 14, the wetting phase diagrams of these inert gases are now readily obtained in Figs. 1–4, respectively. These diagrams should be compared to those for He (Ref. 1) and  $\text{H}_2$ .<sup>5</sup> In each of these diagrams, a given substrate is represented by a point in the  $C_3 - D$  plane. At a specified value of  $T$ , the equality in Eq. (3) yields a curve in this plane; the substrates in the region above (below) such a line are predicted to be wet (nonwet) by the film at the given value of  $T$ . A series of these “isowets” can then be drawn for different temperatures ( $T_t \leq T < T_c$ ).

All of the diagrams show a close similarity in both the relative positions of the substrates and the “isowet” curves, despite the difference in the scales of  $C_3$  and  $D$ . We observe that most well-studied surfaces, such as noble

TABLE I. The values of  $C_3$  (in  $\text{K} \text{Å}^3$ ) for inert gases on various surfaces. The data for non-alkali-metal surfaces are taken from Ref. 13, while those on alkali metals are calculated by us with the method described in Ref. 5.

Surfaces	Ne	Ar	Kr	Xe
Graphite	4020	14000	20100	28500
KCl	2210	7540	10800	15200
LiF	2230	7530	10200	14500
MgO	3770	12100	17100	29900
NaCl	2550	8680	12200	17100
NaF	1720	5790	8120	11700
Ag	6030	19400	27500	37900
Au	6430	20500	28500	40900
Cu	5660	18800	26600	39300
Li	2210	10400		
Na	2110	8370		
K	1480	6320		
Rb	1300	5790		
Cs	1080	5250		

TABLE II. The values of  $D$  (in K) for inert gases on various surfaces. The data for non-alkali-metal surfaces are taken from Ref. 13, while those on alkali metals are calculated by us with the method described in Ref. 5. The data in parentheses are from Ref. 33.

Surfaces	Ne	Ar	Kr	Xe
Graphite	378	1110	1450	1880
KCl	200	829	1250	2040
LiF	157	812	1090	1780
MgO	272	839	1100	1400
NaCl	221	884	1330	2170
NaF	149	620	936	1530
Ag	159	835	1240	2450
Au	280	987	1390	1940
Cu	144	987	1380	2200
Li	29.6			
Na	28.8			
K	16.9 (17.8)	(109)		
Rb	13.1 (15.7)	(97.4)		
Cs	10.1 (12.7)	(84.5)		

metals, graphite, and MgO, are predicted to be wet by the films below the triple temperatures  $T_t$ . This is consistent with the experimental results<sup>15</sup> that only triple point wetting has been observed in these systems.<sup>16</sup> Only the surfaces of NaF and alkali metals are shown in the figure as having  $T_w > T_t$ . The alkali metals (whose data are incomplete) are particularly good candidates to exhibit the wetting transition above  $T_t$  since they are predicted to have fairly high wetting temperatures; see Figs. 1 and 2. They have so far been shown to be nonwetting or weakly

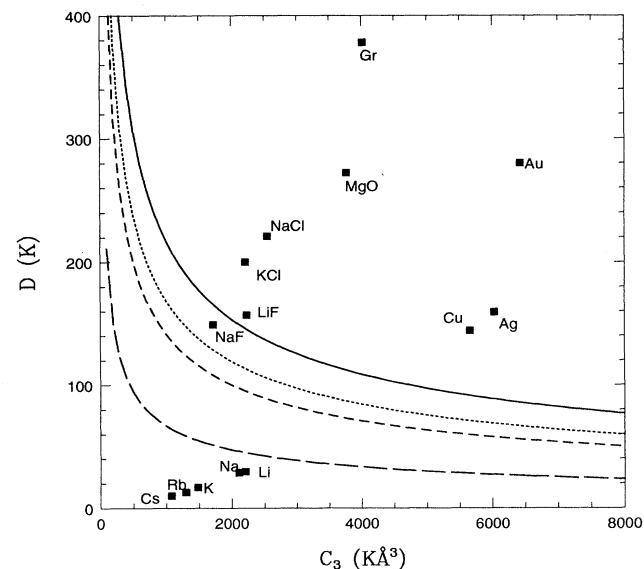


FIG. 1. The wetting phase diagram of liquid Ne films adsorbed on various substrates. Surfaces above a given line are wetted at the specified temperature  $T$ , according to Eq. (3). The solid line is the wetting boundary at triple point  $T_w = T_t = 25$  K and the dotted line is that at  $T_w = 28, 32$ , and  $36$  K. The coordinates  $(C_3, D)$  for substrates are listed in Tables I and II.

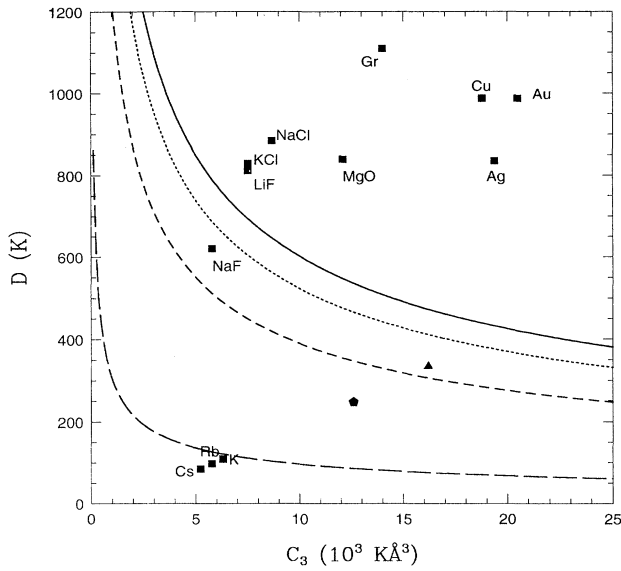


FIG. 2. Same figure as Fig. 1 for liquid Ar films. The solid line is at the triple point  $T_w = T_t = 84$  K. The dot, short dash, and long dash lines are at temperatures  $T_w = 90$ , 100, and 130 K, respectively. The triangle denotes the model Ar/CO<sub>2</sub> system studied in numerical simulations (Refs. 7 and 23), while the pentagon denotes the system found to have  $T_w = 166$  K in Ref. 26.

wetting for <sup>4</sup>He (Ref. 1) and H<sub>2</sub> (Ref. 5) and nonwetting for a few classical gases at very low temperatures.<sup>17,18</sup> The experimental observation of the predicted wetting transition for classical films should thus have significance for our understanding of these phenomena. The availability of surfaces that are not wet by simple fluids above  $T_t$

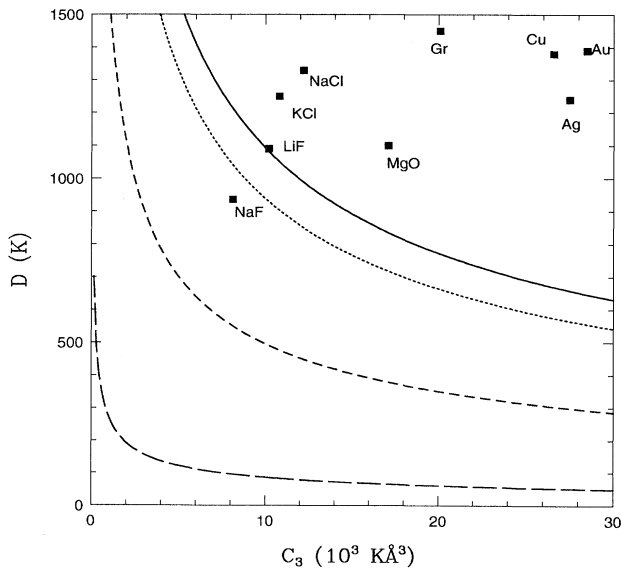


FIG. 3. Same figure as Fig. 1 for liquid Kr films. The solid line is at the triple point  $T_w = T_t = 120$  K. The dot, short dash, and long dash lines are at temperatures  $T_w = 130$ , 160, and 190 K, respectively.

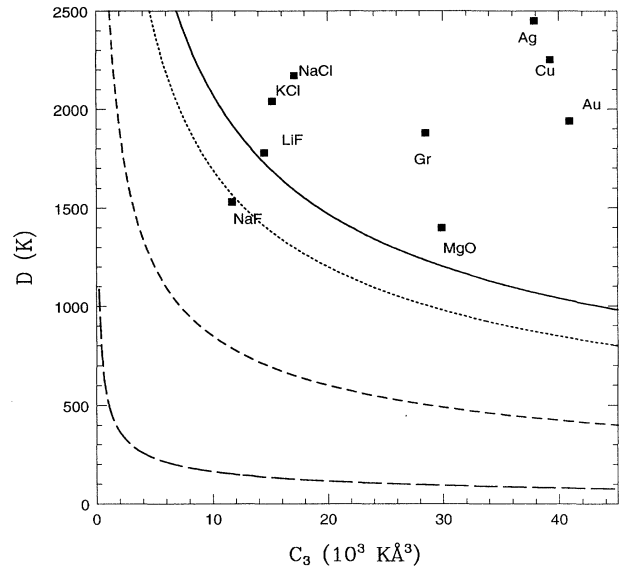


FIG. 4. Same figure as Fig. 1 for liquid Xe films. The solid line is at the triple point  $T_w = T_t = 170$  K. The dot, short dash, and long dash lines are at temperatures  $T_w = 190$ , 220, and 260 K, respectively.

will also make it possible to perform experiments, such as droplet spreading, which are usually done with complex fluids.<sup>19</sup>

In the absence of experimental observation, numerical simulations have traditionally played a very important role in understanding the wetting transitions of simple fluids.<sup>20–24</sup> These include lattice gas and continuum Monte Carlo simulations. A particularly well-studied model system is Ar on a CO<sub>2</sub> surface, with parameters  $C_3 = 16\,400$  K Å<sup>3</sup> and  $D = 334$  K. A wetting temperature of  $T_w = 100$  K has been found in a recent simulation,<sup>23</sup> agreeing with the prediction of our model; see Fig. 2.<sup>25</sup> It has also been shown by a density functional model,<sup>26</sup> that a system with parameters  $C_3 = 12\,600$  K Å<sup>3</sup> and  $D = 247$  K has a wetting temperature  $T_w = 140$  K, compared to 120 K, which our simple model predicts (see Fig. 2).

### III. A NEARLY UNIVERSAL TREND

The qualitative similarity shown in the wetting phase diagrams of Figs. 1–4, as well as those for He and H<sub>2</sub> published earlier, leads to the speculation of a possible scaling form. Indeed, it is worthwhile to note that the *shape* of physical interaction potentials is approximately “universal.”<sup>12,27</sup> Thus they can be written in a reduced form, of which Eq. (2) is the simplest (very) approximate example. Similarly, the adsorbate-adsorbate potential can also be described by two parameters. For later convenience, we choose them to be the well depth  $\epsilon$  and minimum position  $r_m$  of the two-body potential, determining the energy and length scales, respectively. The values of these parameters for inert gases are listed in Table III.<sup>28</sup>

Using these dependences, we observe an approximate universal trend in the interaction parameters. That is, a scaling of the adsorbate-substrate potential by the adsorbate-adsorbate parameters  $\epsilon$  and  $r_m$  gives a nearly common result for the classical inert gases, Ar, Kr, and Xe, as shown in Tables IV and V. In these tables, the parameters  $C_3$  and  $D$  are presented in the following dimensionless form:

$$C_3^* = \frac{C_3}{\epsilon r_m^3}, \quad (4)$$

$$D^* = \frac{D}{\epsilon}. \quad (5)$$

We observe that the average variation in the values of the reduced variables  $C_3^*$  and  $D^*$  for these classical gases is about 20% and 10%, respectively. Note that the scaling variables  $\epsilon$  and  $\epsilon r_m^3$  vary by factors of 2 and 3, respectively, between Ar and Xe. It is thus a reasonable approximation to neglect completely the relatively small variation of  $C_3^*$  and  $D^*$  with adsorbate. This simplification leads to an interesting result. (See Appendix A for a discussion of the origin of this scaling behavior.)

According to the LCS, the thermodynamic properties of classical fluids obey universal relations in reduced form. This is derivable if the only interaction is a pair potential having the scaling form  $\epsilon f(r/r_m)$ ,<sup>8,12</sup> since then  $\epsilon$  and  $r_m$  are the only parameters in the partition function and fully determine the energy and length scales, respectively. It thus leads to the definition of dimensionless surface tension, density, and temperature as

$$\sigma^* = \frac{\sigma_{lv}}{\epsilon/r_m^2}, \quad (6)$$

$$n^* = nr_m^3, \quad (7)$$

and

$$T^* = T/\epsilon. \quad (8)$$

Table III presents values of these quantities at the triple point. Nonuniversality is observed only in the quantum cases.

The wetting condition in Eq. (3) can then be rewritten as

$$(C_3^* D^{*2})^{1/3} = 3.33\sigma^*(T^*)/n^*(T^*). \quad (9)$$

This equation is now universal for all liquid classical films. The important difference between this and Eq. (3) is that here the left side should be independent of adsorbate and the right side is a universal function of  $T^*$ . A “universal” wetting phase diagram is thus possible; we present it in Fig. 5. Its significance is that a given substrate yields the same reduced wetting temperature for all classical gases.

The present application of the LCS to the wetting transition, if verified by experiments, can lead to many useful applications. First of all, such a universality in wetting behavior unifies the qualitative features of quite different systems. Although derived from the properties of simple gases, it is expected to be at least qualitatively true for other, more complex, classical gases such as  $N_2$ ,  $O_2$ , and  $CH_4$ , as in the case of the LCS in bulk classical fluids. It can then serve as a general guide to the prediction of wetting properties, provided that some potential parameters are known. Conversely, one may obtain a reasonable estimation of the adsorption potential from the measured wetting properties of these films.<sup>29,30</sup>

The LCS of classical liquid wetting may be contrasted with predictions based on the application of Eq. (3) to the quantum cases,  $H_2$  and  $^4He$ . For this purpose we show in Fig. 6 the wetting conditions for classical, Ne, and  $H_2$  films at  $T_w^* = T_t^*$  and He at  $T = 0$ . Other systems lie below the classical line for  $T_w^* = T_t^*$ , in the order of increasing de Boer quantum parameter:<sup>8</sup> Ne,  $H_2$ ,  $^4He$ , and  $^3He$ , with Ne being extremely close to the classical one. This indicates that quantum films are better wetting agents than classical ones. This trend can be explained by zero-point motion, which broadens the liquid-vapor interface region and reduces the surface tension  $\sigma_{lv}$ .<sup>20</sup> Such an effect is manifested in the anomalously small values of  $\sigma^*$  for He shown in Table III. In fact the zero-point motion reduces both  $\sigma^*$  and  $n^*$  values, but the ratio  $\sigma^*/n^*$  is still systematically smaller for quantum fluids.<sup>21</sup> According to Eq. (9), this leads to the observation that quantum films are generally better wetting agents than classical ones. What had been recognized previously as an origin of this behavior is that  $\epsilon$  is small, so that  $D$  is typically much larger than  $\epsilon$ . Our point here is that this large value of  $D^*$  is by itself not enough to characterize the phenomenon. The *additional* factor which enhances wetting

TABLE III. The polarizability  $\alpha$  and the well depth  $\epsilon$  and minimum position  $r_m$  of the two-body interaction potentials of noble gases. Also listed are values of their triple temperature  $T_t^*$ , liquid-vapor surface tension  $\sigma^*$ , bulk liquid density  $n^*$ , and their ratio at  $T_t^*$ , all in reduced units defined in the text. The values  $\epsilon$  and  $r_m$  are from Ref. 27 while the numbers of  $n^*$  and  $\sigma^*$  are calculated from original data in Ref. 14.

Gas	$\epsilon$ (K)	$r_m$ (Å)	$\alpha$ (Å <sup>3</sup> )	$T_t^*$	$n^*(T_t^*)$	$\sigma^*(T_t^*)$	$\sigma^*(T_t^*)/n^*(T_t^*)$
$^3He$	10.8	2.97	0.205	0.00	0.43	0.09	0.21
$^4He$	10.8	2.97	0.205	0.00	0.58	0.21	0.36
$H_2$	34.3	3.41	0.806	0.40	0.98	0.70	0.71
Ne	42.3	3.08	0.396	0.58	1.07	0.89	0.83
Ar	143.2	3.76	1.642	0.58	1.12	0.96	0.86
Kr	199.9	4.01	2.487	0.58	1.13	0.94	0.83
Xe	282.3	4.36	4.012	0.57	1.13	0.93	0.82

TABLE IV. The values of  $C_3^*$  for inert gases on various surfaces. The original data are taken from Table I and Ref. 13. The values of  $C_{cl}^*$  are the average for classical gases Ar, Kr, and Xe and the error is the relative statistical error of the average.

Gases	Gr	KCl	LiF	MgO	NaCl	NaF	Ag	Au	Cu
He	7.38	3.81	3.81	6.19	4.35	2.99	10.21	11.23	9.64
H <sub>2</sub>	4.44	2.34	2.23	3.17	2.64	1.86	6.09	6.56	5.88
Ne	3.25	1.79	1.80	3.05	2.06	1.39	4.88	5.20	4.58
Ar	1.84	0.99	0.95	1.59	1.14	0.76	2.55	2.69	2.47
Kr	1.56	0.84	0.79	1.33	0.95	0.63	2.13	2.21	2.06
Xe	1.22	0.65	0.62	1.28	0.73	0.50	1.62	1.75	1.68
$C_{cl}^*$	1.54	0.83	0.79	1.40	0.94	0.63	2.10	2.22	2.07
error (%)	17	17	17	9.8	18	17	18	17	16

is the quantum effect of a depressed  $\sigma^*/n^*$ , manifested in the difference between the classical and quantum curves in Fig. 6.

#### IV. DISCUSSION

We should emphasize that we do *not* intend to present here a rigorous theory of either the universal trend in the physical interactions or the extension of the LCS to wetting phenomena. We do believe, however, that the observations and conclusions we present should be at least qualitatively valid. These conclusions have potentially significant impact on the study of interaction potentials and wetting transitions. Quantitative predictions, on the other hand, are limited by several factors. One is our incomplete knowledge of the adsorption potentials. The other is our oversimplification of the statistical mechanics. The simple model leading to Eq. (3) is based on a relatively crude free energy balance. Its applicability at higher temperature is yet to be tested thoroughly, although recent evidence indicates that it works very well for liquid H<sub>2</sub> wetting above its triple temperature 14 K.<sup>5</sup> Approximations are also implicit in the neglect of detailed information about the film density profile, especially near the interfaces. Other corrections to the energy balance are also possible, including substrate zero-point phonon effects;<sup>31</sup> this is important for quantum films, but not for classical ones (because of the much higher characteristic energy scale in the latter case).

It is possible and desirable to improve upon our simple model by using more sophisticated techniques such as a

density functional model or numerical simulations.<sup>6,23,24</sup> Such an extension will also enable us to study the behavior of films with a finite thickness (away from coexistence), where prewetting transitions occur.

In summary, we have presented an extension of the LCS to the case of wetting transitions of classical liquid films. We have also shown that quantum motion is one of the major factors (along with a weak two-body interaction) for the better wetting property of quantum films. Our extension, if confirmed by experiments, should be of great interest and importance in the study of wetting and phase transitions in general.

#### ACKNOWLEDGMENTS

We are indebted to C. Carraro, M. H. W. Chan, G. Mistura, M. Swift, and F. Toigo for many helpful discussions throughout this work. E.C. wishes to thank the Direction de la Recherche et des Etudes Doctorales of France for support. This research has been supported in part by National Science Foundation Grants No. DMR-9022681 and No. DMR-9014679 and the Petroleum Research Fund of the American Chemical Society.

#### APPENDIX A: SCALING OF INTERACTION PARAMETERS

In the text it is observed that  $C_3^*$  and  $D^*$  depend only weakly on the adsorbate, for a given substrate and a classical gas. The origin of this approximately universal

TABLE V. The values of  $D^*$  for inert gases on various surfaces. See Table IV caption.

Gases	Gr	KCl	LiF	MgO	NaCl	NaF	Ag	Au	Cu
He	17.8	9.77	9.13	8.06	6.55	8.14	6.44	8.59	6.74
H <sub>2</sub>	17.5	11.8	—	16.2	2.65	8.90	10.7	13.5	7.44
Ne	8.94	4.72	3.70	6.42	4.99	3.53	3.76	6.61	3.40
Ar	7.78	5.79	5.67	5.86	6.17	4.33	5.83	6.89	6.89
Kr	7.25	6.27	5.47	5.50	6.67	4.68	6.21	6.96	6.91
Xe	6.66	7.23	6.29	4.97	7.68	5.42	8.67	6.87	7.81
$D_{cl}^*$	7.23	6.43	5.81	5.45	6.84	4.81	6.90	6.91	7.20
error (%)	6.3	9.3	6.0	6.7	9.2	9.5	18.2	0.6	6.0

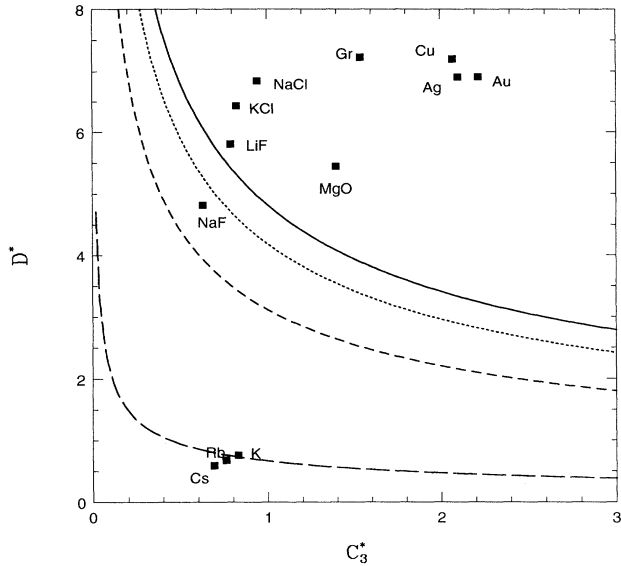


FIG. 5. The “universal” wetting phase diagram of classical liquid films adsorbed on various substrates. Surfaces above a given line are wetted at the specified reduced temperature  $T^*$ , according to Eq. (9). The solid line is at the triple point  $T_w^* = T_t^* = 0.58$ . The dot, short dash, and long dash lines are at temperatures  $T_w^* = 0.63, 0.70$ , and  $0.91$ , respectively. The squares illustrate positions of substrates whose coordinates are  $(C_{cl}^*, D_{cl}^*)$  as listed in Tables IV and V. The positions of K, Rb, and Cs are drawn with the data for Ar only.

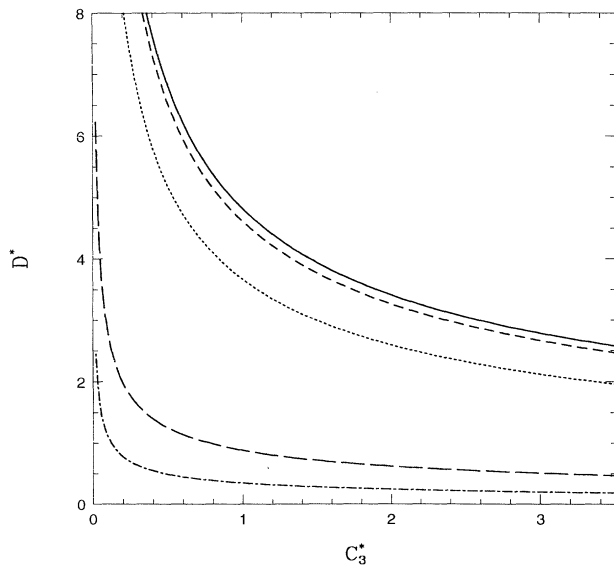


FIG. 6. The wetting lines of classical liquid films (solid line), Ne films (short dash line), and  $H_2$  film (dot line), all at triple temperature, and that of the  $^4He$  (long dash line) and  $^3He$  films at zero temperature (dot-dash line).

behavior can be understood qualitatively from empirical and theoretical knowledge of physical interactions. First, consider  $D^* = D/\epsilon$ . An adsorption potential law of corresponding states has been shown to be valid, yielding<sup>27</sup>

$$D \simeq \frac{C_3}{(z_m + \lambda)^3}, \quad (A1)$$

where  $\lambda$  is a distance of order  $0.5 \text{ \AA}$  characterizing the decay of the substrate charge density outside of the surface. Next, it has been shown that the adsorption dispersion coefficient satisfies<sup>32</sup>

$$C_3 \simeq \frac{G\alpha}{1 + E_s/E_a}, \quad (A2)$$

where  $\alpha$  is the adsorbate polarizability,  $G$  is a substrate-dependent constant, and the energies  $E_s$  and  $E_a$  are characteristic of the substrate and adsorbate. Hence for a given substrate

$$D^* \simeq \left(\frac{\alpha}{\epsilon}\right) \frac{G}{(1 + E_s/E_a)(z_m + \lambda)^3}. \quad (A3)$$

Figure 7 shows that  $\alpha/\epsilon$  is roughly a constant for the gases of interest. Similarly weak in its dependence on adsorbates is the energy term in the denominator. Finally, the distance term is also fairly insensitive to adsorbates, even though cubed, because the equilibrium distance is largely determined by the substrate charge density. The relatively small residual dependence of  $D^*$  on adsorbates is a consequence primarily of this distance

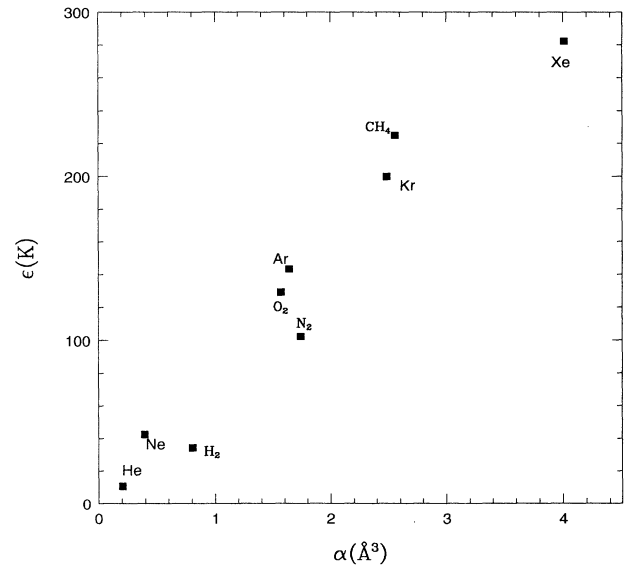


FIG. 7. The two-body interaction well depth  $\epsilon$  as a function of the atomic (molecular) polarizability  $\alpha$  for simple gases. The data are taken from Ref. 12, some of which are listed in Table III.

variation. Atoms with smaller sizes such as He, Ne, and  $\text{H}_2$  are observed to have systematically larger values of  $D^*$ .

We turn next to  $C_3^*$ . From its definition, Eq. (4), and Eqs. (A2) and (A3), we find

$$C_3^* \simeq D^* \left( \frac{r_m}{z_m + \lambda} \right)^3. \quad (\text{A4})$$

Note that the factor multiplying  $D^*$  involves the ratio of two lengths. Since each of these grows with atomic number  $A$ , there is a tendency for the resulting  $C_3^*$  to vary with  $A$  the same way  $D^*$  does, i.e., very little. The skeptical reader will doubtlessly regard this heuristic analysis as a rationalization of empirical data. The argument presented here, however, is not essential to establishing the main points made in the text, which are based on the numbers themselves.

- <sup>1</sup>E. Cheng, M. W. Cole, W. F. Saam, and J. Treiner, Phys. Rev. Lett. **67**, 1007 (1991); Phys. Rev. B **46**, 13 967 (1992); **47**, 14 661(E) (1993); E. Cheng, M. W. Cole, J. Dupont-Roc, W. F. Saam, and J. Treiner, Rev. Mod. Phys. **65**, 557 (1993); M. W. Cole, E. Cheng, C. Carraro, W. F. Saam, M. R. Swift, and J. Treiner, Physica B (to be published).
- <sup>2</sup>P. J. Nacher and J. Dupont-Roc, Phys. Rev. Lett. **67**, 2966 (1991); N. Bigelow, P. J. Nacher, and J. Dupont-Roc, J. Low Temp. Phys. **89**, 135 (1992).
- <sup>3</sup>K. S. Ketola, S. Wang, and R. B. Hallock, Phys. Rev. Lett. **68**, 201 (1992); S. K. Mukherjee, D. P. Druist, and M. H. W. Chan, J. Low Temp. Phys. **87**, 113 (1992).
- <sup>4</sup>P. Taborek and J. E. Rutledge, Phys. Rev. Lett. **68**, 2184 (1992); J. E. Rutledge and P. Taborek, *ibid.* **69**, 937 (1992); P. Taborek and J. E. Rutledge, *ibid.* **71**, 263 (1993); M. Schick and P. Taborek, Phys. Rev. B **46**, 7312 (1992).
- <sup>5</sup>E. Cheng, G. Mistura, H. C. Lee, M. H. W. Chan, M. W. Cole, C. Carraro, W. Saam, and F. Toigo, Phys. Rev. Lett. **70**, 1854 (1993); G. Mistura, H. C. Lee, and M. H. W. Chan, Physica B (to be published).
- <sup>6</sup>S. Dietrich, in *Phase Transitions and Critical Phenomena*, edited by C. Domb and J. L. Lebowitz (Academic Press, San Diego, 1988), Vol. 12; M. Schick, in *Liquids at Interfaces*, edited by J. Charvolin, J. F. Joanny, and J. Zinn-Justin (Elsevier, Amsterdam, 1990).
- <sup>7</sup>C. Ebner and W. F. Saam, Phys. Rev. Lett. **38**, 1486 (1977); J. W. Cahn, J. Chem. Phys. **66**, 3667 (1977).
- <sup>8</sup>See, for example, R. K. Pathria, *Statistical Mechanics* (Pergamon, Oxford, 1972).
- <sup>9</sup>An equivalent condition for the Ising lattice gas model is given in W. F. Saam, Surf. Sci. **125**, 253 (1983).
- <sup>10</sup>An alternative to the approximation  $\hat{\sigma}_{sl}(T) = \sigma_{lv}(T)$  is to use  $\hat{\sigma}_{sl}(T) = \sigma_{lv}(T_t)$ , i.e., a constant value taken at the triple temperature. This would better account for the stiffness of the solid-vapor interface and reduce the predicted value of  $T_w$  slightly for  $T \sim T_w$ . However, the error of this approximation becomes more pronounced at higher temperatures.
- <sup>11</sup>The choice of the potential form here is purely for mathematical convenience. Using other forms would result in only a small modification in the coefficient on the right-hand side of Eq. (3). This was shown explicitly in the case of  $\text{H}_2$  on alkali metals (Ref. 5), for which the integral in Eq. (1) was typically 10% too small in magnitude when Eq. (2) was used instead of the theoretical potentials.
- <sup>12</sup>R. A. Aziz, in *Inert Gases*, edited by M. L. Klein (Springer, Berlin, 1984), and references therein.
- <sup>13</sup>G. Vidali, G. Ihm, H. Y. Kim, and M. W. Cole, Surf. Sci. Rep. **12**, 135 (1991), and references therein.
- <sup>14</sup>R. K. Crawford, in *Rare Gas Solids*, edited by M. L. Klein and J. A. Venables (Academic, London, 1977), Vol. II, Chap. 11; N. B. Vargaftik, *Tables on the Thermophysical Properties of Liquids and Gases* (Hemisphere, Washington, D.C., 1975); B. A. Younglove, J. Phys. Chem. Ref. Data **11**, Suppl. 1 (1982); S.-T. Wu and G.-S. Yan, J. Chem. Phys. **77**, 5799 (1982), and references therein.
- <sup>15</sup>J. Krim, J. G. Dash, and J. Suzanne, Phys. Rev. Lett. **52**, 640 (1984); M. Dirr and G. B. Hess, Phys. Rev. B **33**, 4758 (1986); A. D. Migone, J. G. Dash, M. Schick, and O. E. Vilches, *ibid.* **34**, 6322 (1986); G. Zimmerli and M. H. W. Chan, *ibid.* **45**, 9347 (1992).
- <sup>16</sup>The wetting transition below  $T_i$  is presumably prevented from being observed by the lattice mismatch effect present with solid films.
- <sup>17</sup>R. A. Pierotti and G. D. Halsey, Jr., J. Phys. Chem. **63**, 680 (1959); M. Onellion and J. L. Erskine, Surf. Sci. **177**, L983 (1986); E. Lerner, R. Morley, and O. E. Vilches, J. Low Temp. Phys. **89**, 953 (1992); W. Friess, E. Steinacker, T. Brunner, and D. Menzel (unpublished); D. Menzel (private communication).
- <sup>18</sup>The alkali-metal surfaces are weakly binding for inert gases because of their relatively large decay length of electron density outside the surface which repels atoms (molecules) with closed shell electrons; see Ref. 13.
- <sup>19</sup>P. Ball, Nature (London) **338**, 624 (1989); F. Heslot, N. Fraysee, and A. M. Cazabat, *ibid.* **338**, 640 (1989).
- <sup>20</sup>W. Saam and C. Ebner, Phys. Rev. Lett. **34**, 253 (1975); Phys. Rev. B **12**, 923 (1975).
- <sup>21</sup>In the case of nuclear matter, taking a well depth  $\epsilon$  of about 50 MeV, a minimum radius  $r_m$  of 1 fm, a surface tension  $\sigma$  of 1 MeV/fm<sup>2</sup>, and a number density  $n$  of 0.16 fm<sup>-3</sup>, one finds that  $\sigma^*/n^* = 0.125$ . This value, smaller than that of <sup>3</sup>He, is consistent with the quantum influence we discuss here, although the nuclear interaction is of a different nature than the interatomic one.
- <sup>22</sup>R. Pandit, M. Schick, and M. Wortis, Phys. Rev. B **26**, 5112 (1982).
- <sup>23</sup>J. F. Finn and P. A. Monson, Phys. Rev. A **39**, 6402 (1989).
- <sup>24</sup>R. Evans, in *Liquids at Interfaces*, edited by J. Charvolin, J. F. Joanny, and J. Zinn-Justin (Elsevier, Amsterdam, 1990).
- <sup>25</sup>The truncated two-body interaction used in the simulation in Ref. 23 has an effective well depth  $\epsilon_{\text{eff}}$  larger than the value  $\epsilon$  used in scaling. For example, their critical point has  $T_c = 147$  K, compared to the Lennard-Jones liquid value of 162 K. This should result in smaller  $C_3$  and  $D$  values for our comparison in Fig. 2.
- <sup>26</sup>E. Bruno, C. Caccamo, and P. Tarazona, Phys. Rev. A **35**, 1210 (1987).
- <sup>27</sup>The reduced potential for adsorption differs, of course, from that of the interatomic interactions. See G. Vidali, M. W.

Cole, and J. R. Klein, Phys. Rev. B **28**, 3064 (1983); G. Ihm, M. W. Cole, F. Toigo, and G. Scoles, J. Chem. Phys. **87**, 3995 (1987).

<sup>28</sup>A convenient and widely used form of a two-parameter potential is that of the Lennard-Jones 6-12 form with energy and length parameters  $\epsilon_{\text{LJ}}$  and  $\sigma_{\text{LJ}}$ . Typically,  $\epsilon_{\text{LJ}}$  values underestimate the real well depth  $\epsilon$  by 15%; see Ref. 12.

<sup>29</sup>W. F. Saam, J. Treiner, E. Cheng, and M. W. Cole, J. Low

Temp. Phys. **89**, 637 (1992).

<sup>30</sup>We have used the experimental values  $\sigma(T)$  and  $n(T)$  of Ar (Ref. 14) in place of  $\sigma^*(T^*)$  and  $n^*(T^*)$ , respectively, for the calculation.

<sup>31</sup>M. W. Cole, M. R. Swift, and F. Toigo, Phys. Rev. Lett. **69**, 2682 (1992).

<sup>32</sup>G. Vidali and M. W. Cole, Surf. Sci. **110**, 10 (1981).

<sup>33</sup>A. Chizmeshya (private communication).